

The Shadow Path integral Ground State method: New light into the Physics of Quantum Solids

Ettore Vitali (*), Davide Emilio Galli (*), Luciano Reatto(*)

Dipartimento di Fisica, Università degli Studi di Milano, via Celoria 16, 20133, Milano ()*

(Received on December 19, 2006)

Abstract

A causa della piccola massa degli atomi e della debole interazione tra di essi, un campione di atomi di ^4He costituisce un prototipo di quello che viene solitamente definito solido quantistico, cioè un solido i cui atomi, grazie al moto di punto zero, compiono delle oscillazioni di notevole ampiezza attorno alle relative posizioni reticolari esplorando una vasta regione della cella elementare. Ciò dà luogo a uno scenario in cui divengono possibili processi quali scambi tra le particelle e delocalizzazione di difetti, che possono rendere “visibili” a livello macroscopico le leggi della meccanica quantistica che governano la fisica del sistema. Attraverso una tecnica Monte Carlo, il metodo “shadow path integral ground state”, che rende possibile il calcolo esatto di alcune proprietà del sistema a $T=0$ K, stiamo indagando la fisica del sistema in presenza di vacanze, difetti puntuali che potrebbero giocare un ruolo molto importante in una possibile transizione a una fase supersolida.

Due to the small masses of the atoms and the weak interatomic binding, solid ^4He is a prototype of what is called a quantum solid, that is a solid in which atoms, due to their zero-point motion, execute very large amplitude vibrations around their lattice sites and explore a sizeable fraction of the primitive cells. This fact opens a scenario in which processes like exchanges between particles or delocalized defects are allowed; such processes could in principle allow one to observe, in a macroscopic domain, phenomena displaying the fundamental laws of Quantum Mechanics which governs the microphysics of the system. By means of a Monte Carlo technique, the Shadow Path Integral Ground State method, which allows one to evaluate exact properties of the $T=0\text{K}$ physics of the system, we are studying the properties of the system when vacancies are present; such point-defects could play a very important role in a probable transition to a “supersolid” phase.

Keywords: Supersolid; Quantum solids; Monte Carlo methods.

1. Introduction. ^4He , quantum solid.

The study of condensed phases of ^4He has played a very important role in the context of modern condensed matter Physics, both providing an extremely interesting experimental scenario, allowing one to see quantum effects in a macroscopic system, and being a constant test case of many body-theories and of computational methods. In fact the system, though possessing all the features of a strongly interacting one, does not have the added complexities related to Fermi statistics or to nuclear Physics, and so it is possible to describe it, with a great accuracy level, from “first principles”, starting from a microscopic Hamiltonian, and to investigate its properties, on a quantitative basis, using “Quantum Monte Carlo” computational methods. From both a theoretical and an experimental point of view, the striking properties of the “permanent liquid” ^4He , known under the name of “phenomenon of superfluidity”, have been extensively studied during last decades and computational methods have provided the possibility of giving a deep insight into the properties of the system. In fact, using such methods, it has been possible to clarify the physical origins of this very peculiar behavior of liquid Helium below the “lambda” transition, realizing that such a macroscopic behavior is deeply connected with the quantum nature of the Helium particles: Bose indistinguishability. Besides, it has been possible to put light into the very old question whether superfluidity of ^4He could be in some way related to Bose Einstein Condensation (BEC), very famous in the realm of the physics of cold, diluted Bose gases. BEC, in fact, and ODLRO (the equivalent of BEC for interacting systems), are due to exchange effects, which at low temperature become very important.

It is known that ^4He , under the external pressure of $P \cong 25 \text{ atm}$, at $T = 0 \text{ K}$, becomes a solid; such a pressure, in fact, is sufficient to stabilize a crystalline order which, at $P = 0 \text{ atm}$, is destroyed by the zero-point motion of the Helium atoms. Since 1970 [1] it has been argued that even in a crystalline phase, with broken translational symmetry, it could be possible to observe quantum coherence phenomena, such as BEC and superfluidity. One can imagine a physical picture in which particles localization, induced by the crystalline order, has to find a compromise with particles delocalization, due to the light mass, and hence to the high zero-point kinetic energy of Helium atoms. It is not difficult to realize that, if the zero-point motion, maybe coupled to some defects in the system [2][1], as we will discuss in some detail later, is large enough to let the atoms explore sizeable fractions of the unit cells of the crystal lattice, particles can exchange their positions, making Bosonic indistinguishability play a crucial role, and this, in principle, could lead to a “supersolid” state of matter, that is a solid in which quantum

coherence effects (namely BEC and superfluidity) are present. For many years no experimental evidence of such a supersolid state was found, till 2003, when, in some experiments performed by Chan *et al.* [3], a drop in the rotational inertia of solid ^4He , bulk and confined in porous media, was observed below a certain critical temperature; this “non-classical rotational inertia” could be interpreted as a superfluid behavior in solid Helium, “supersolidity”. Because of this experiment, the first *probable* (there is no general agreement about the interpretations of these experiments) experimental evidence of a supersolid phase, the interest in studying solid phases of ^4He has very recently gained strong importance and accurate simulations methods, quantum Monte Carlo methods, which work so well when dealing with liquid Helium, make possible to predict on a quantitative basis the physical properties of a quantum solid.

In the following sections, we are going to introduce the Quantum Monte Carlo method which we use in our calculations of solid Helium properties, the *Shadow Path Integral Ground State* (SPIGS) method, recently developed [4], which opens the possibility to study by exact methods at $T=0K$ the physics of ^4He . In order to clarify the physical motivations of this method, it is useful to discuss first the variational *Shadow Wave Function* (SWF) technique [5], that is a very accurate variational model of the ground state of a collection of interacting bosons, from which, as we shall see, SPIGS method projects out the true ground state.

2. Shadow Wave Functions and Shadow Path Integral Ground State methods

When studying the bulk properties of ^4He atoms the internal structure of the atoms can be neglected and it is a very good approximation to describe the system as a collection of structureless and spinless bosons, with an effective Hamiltonian of the form:

$$\hat{H} = -\frac{\hbar^2}{2m} \sum_{i=1}^N \nabla_i^2 + \sum_{i<j=1}^N v(|\vec{\hat{r}}_i - \vec{\hat{r}}_j|) \quad (2.1)$$

Writing this Hamiltonian, it is assumed that the potential energy can be written in terms of a pair additive central potential $v(r)$, which is the only phenomenological input in the description of the system by means of Quantum Monte Carlo methods. $v(r)$ is very large and positive at short distance, corresponding to a large repulsive inter-atomic force, due to

Pauli exclusion principle; beyond a distance of order of 2.5\AA , $v(r)$ becomes negative and there is an attractive well due to Van der Waals forces. A simple approximation for $v(r)$ is the Lennard-Jones potential, but more accurate representations of $v(r)$ are known [6].

In order to put light into the zero temperature physics of the system, whose strong interaction does not allow any perturbative treatment, it is necessary to build up a variational model of the ground state of (2.1), in which correlations among the particles have to play a very important role.

The SWF technique [5] is a variational theory based on a trial wave function in which inter-particle correlations are introduced both explicitly, via a two-body pseudopotential, and implicitly via a coupling between the particles and subsidiary variables which are integrated over. The original motivation was to obtain a wave function which is translationally invariant and, at the same time, it can describe the solid phase without assuming a priori equilibrium positions. In addition to the set $R = (\vec{r}_1, \dots, \vec{r}_N)$ of positions of the particles, in the SWF technique it is introduced a second set $S = (\vec{s}_1, \dots, \vec{s}_N)$ of variables, which are called shadows: the wave function is written in the following implicit form:

$$\psi_{sh}(R) = \int dS \phi(R) K(R, S) \phi_s(S) \quad (2.2)$$

where $\phi(R) = \prod_{i < j=1}^N e^{-\frac{1}{2}u(r_{ij})}$ contains the explicit part of the inter-particle

correlations, which are assumed of the Jastrow form (only two-body correlations are present), $K(R, S)$ is usually taken as a product of

Gaussians $K(R, S) = \prod_{i=1}^N e^{-C|\vec{r}_i - \vec{s}_i|^2}$ which correlates each real variable

with a shadow variable, and $\phi_s(S)$ in another Jastrow factor which takes into account the inter-shadow correlations. In the wave functions (2.2) it can be shown that implicit correlations induced by the integration over the subsidiary shadow variables are of the order of the number of particles N . A formal way to understand the SWF functional form is the following: let us consider a Jastrow wave function:

$$\phi(R) = \prod_{i < j=1}^N e^{-\frac{1}{2}u(r_{ij})} \quad (2.3)$$

where $u(r)$ is a function which must be variationally optimized; the wave function (2.3) is the simplest way of introducing inter-particle correlations in a translationally invariant bosonic system. As it can be shown that (2.3) has non zero overlap with the true ground state $\Psi_0(\vec{r}_1, \dots, \vec{r}_N)$ of the system, than it is a geometrical property of the Hilbert space of the system the fact that:

$$\begin{aligned}\psi_0(R) &= \lim_{\tau \rightarrow +\infty} \int dR' G(R, R'; \tau) \phi(R') \\ G(R, R'; \tau) &\stackrel{\text{def}}{=} \left\langle R \left| e^{-\hat{H}\tau} \right| R' \right\rangle\end{aligned}\quad (2.4)$$

Unfortunately $G(R, R'; \tau)$ for large τ is not known; however it is possible to improve the Jastrow description applying the imaginary time propagator $G(R, R'; \tau)$ for a small value of τ to $\phi(R)$: in fact the following *primitive* approximation is at hand:

$$\begin{aligned}G(R, R'; \tau) &\underset{\tau \rightarrow 0}{\approx} e^{-\frac{\tau}{2}V(R)} \left(\frac{m}{2\pi\hbar^2} \right)^{\frac{3}{2}N} \prod_{i=1}^N e^{-\frac{m}{2\hbar^2} |\vec{r}_i - \vec{r}'_i|^2} e^{-\frac{\tau}{2}V(R')} \\ V(R) &= \sum_{i < j=1}^N v(r_{ij})\end{aligned}\quad (2.5)$$

If one uses this approximation, it is very easy to see that the functional form of the resulting wave function is exactly the SWF form in eq. (2.2). So a SWF can be seen as a first projection step on the true ground state operated with an imaginary time propagator in the primitive approximation; in order to make this first projection step as efficient as possible it is useful to replace $V(R), V(R')$ and the exponent of the Gaussians in (2.5) by “pseudopotentials” which contain variational parameters that can be optimized via the variational principle for the expectation value of the Hamiltonian.

We are not going here to enter the details of VMC methods, that is Monte Carlo methods which use shadow wave functions, because such methods can be seen as a very special kind of SPIGS method, which we will describe below. SWF technique is so efficient that one is able to describe the solid and liquid phases of Helium with the same functional form. The energies of both phases are comparable in accuracy and quite good, although we are still at a variational level.

Now, it is possible to improve the description of the ground state of (2.1) using (2.4) and the very important factorization property:

$$e^{-(\tau+\tau')\hat{H}} = e^{-\tau\hat{H}} e^{-\tau'\hat{H}} \quad (2.6)$$

Starting from a SWF and adding successive “small” projection steps in imaginary time propagation, it is possible to “reach” the true ground state of the system; in fact, from (2.4) and (2.6), one can write:

$$\begin{aligned} \psi_0(R) &= \lim_{M \rightarrow +\infty} \int dS dR_0 \dots dR_{M-1} G(R, R_{M-1}; \delta\tau) G(R_{M-1}, R_{M-2}; \delta\tau) \dots \\ &G(R_1, R_0; \delta\tau) \phi(R_0) K(R_0, S) \phi_s(S) \\ \delta\tau &\equiv \frac{\tau}{M} \end{aligned} \quad (2.7)$$

where $\delta\tau$ is sufficiently small that approximation (2.5) for $G(R, R_{M-1}; \delta\tau)$ (even more refined approximations are known [7],[8]) is accurate. This synthesizes what is done in the SPIGS, Shadow Path Integral Ground State, method. One uses the wave function:

$$\begin{aligned} \psi_{SPIGS}(R) &= \int dS dR_0 \dots dR_{M-1} G(R, R_{M-1}; \delta\tau) G(R_{M-1}, R_{M-2}; \delta\tau) \dots \\ &G(R_1, R_0; \delta\tau) \phi(R_0) K(R_0, S) \phi_s(S) \\ \delta\tau &\equiv \frac{\tau}{M} \end{aligned} \quad (2.8)$$

which, if τ is large enough, is a very good approximation of the true ground state of the system.

It is clear from (2.8) that the SPIGS wave function rises from the imaginary time evolution of the shadow wave function; in the Hilbert space of the system, such a dynamics defines a curve which approaches the true ground state of the system. Using (2.6) we have discretized this path in steps, short enough in order to control the approximations; in the following, we will call “time slices” these steps.

The possibility of making calculations using the wave function (2.8) is provided by an extremely useful mapping from the quantum mechanics of the ground state of a collection of interacting bosons into the classical statistical mechanics of a fluid of polymers in thermal equilibrium, in the canonical ensemble. To see this, let us write down the expectation value

of an operator which is diagonal in the coordinate representation, $\hat{O} = \hat{O}(\hat{R})$:

$$\frac{\langle \psi_{SPIGS} | \hat{O} | \psi_{SPIGS} \rangle}{\langle \psi_{SPIGS} | \psi_{SPIGS} \rangle} = \int dR_0 \dots dR_{2M} dS dS' p(R_0, \dots, R_{2M}, S, S') O(R_M) \quad (2.9)$$

where:

$$p(R_0, \dots, R_{2M}, S, S') = \frac{\phi_s(S) K(S, R_0) \phi(R_0) \prod_{i=0}^{2M-1} G(R_i, R_{i+1}; \delta\tau) \phi(R_{2M}) K(R_{2M}, S') \phi_s(S')}{\int dR_0 \dots dR_{2M} dS dS' \phi_s(S) K(S, R_0) \phi(R_0) \prod_{i=0}^{2M-1} G(R_i, R_{i+1}; \delta\tau) \phi(R_{2M}) K(R_{2M}, S') \phi_s(S')} \quad (2.10)$$

The average in (2.9) is therefore equivalent to a canonical average of a classical system of linear polymers and it can be computed by using standard Monte Carlo simulation techniques developed for classical systems. In particular, we use the standard Metropolis algorithm in order to sample the probability (2.10); multilevel moves [7] together with single particle moves and global moves are used for guarantee the ergodicity of the sampling algorithm. Once we have chosen an accurate approximation of the imaginary time propagator $G(R_i, R_{i+1}; \delta\tau)$ at short time step, such as the primitive approximation (2.5), or even more refined approximations (the pair product approximation [7] or the Suzuki-Chin approximation [8]), (2.10) is the Boltzmann thermal statistical weight defined on the $3N(2M+3)$ -dimensional configurational space of “special” interacting open polymers. We have used the word “special” because, if one writes down explicitly (2.10) using the primitive approximation, he sees that the interactions of these polymers are very peculiar: inter-polymer interaction is present only between particles belonging to the same time slice. This property is very useful when one deals with (2.10) by means of computer simulation methods, because, even if each polymer is composed by a large number of atoms (one has to notice that, in order to “reach” the true ground state of the system, we need a large number of atoms in the polymers), each monomer interacts only with the others $N-1$ belonging to the same time slice, and this fact reduces significantly the computational effort.

It is worth realizing that the Bose symmetry is already contained in the shadow wave function, so we don't need to worry about the difficulties connected with sampling permutations, with which one has to deal by using PIMC (Path Integral Monte Carlo) method [7].

3. Calculations of Helium properties with SPIGS

The quantum-classical mapping discussed above allows one to use classical Monte Carlo methods to evaluate quantum expectation values like (2.9): we use the Metropolis algorithm.

To be more precise, we explore the configurational space of the classical polymers by means of a random walk, which, asymptotically, gives rise to configurations which are distributed according to the statistical weight $p(R_0, \dots, R_{2M}, S, S')$ given by (2.10); by means of these configurations, the law of large numbers allows one to evaluate integrals like (2.9), with, at least in principle, controllable statistical errors. In this way, one is able to study all configurational properties of Helium, both in the liquid and in the solid phase; for example the pair correlation functions $g(\vec{r}_1, \vec{r}_2)$ and the static structure factor $S(\vec{k})$, which reveal, in the study of the solid phase or of the liquid-to-solid phase transition, the details of the crystalline structure of the system and can give important informations about the presence of defects in the system. This is very interesting because such defects could play a very important role in a probable solid-to-supersolid transition.

It is obviously also possible to evaluate the local density of particles, correlations of particle with impurities (such as an ^3He atom) and so on. Besides, it is possible to evaluate also the energy of the system; in fact, despite the fact that the Hamiltonian is not diagonal in coordinate representation, it commutes with the imaginary time evolution operator $e^{-\tau\hat{H}}$, and so, as one immediately sees, it is possible to construct a “local energy estimator”, defined on the polymers configurational space:

$$E_L(R_0, R_{2M}, S, S') = \frac{1}{2} \left\{ \frac{(\hat{H}K(S, R_0)\phi(R_0))}{K(S, R_0)\phi(R_0)} + \frac{(\hat{H}K(R_{2M}, S')\phi(R_{2M}))}{K(R_{2M}, S')\phi(R_{2M})} \right\} \quad (3.1)$$

and to write:

$$\frac{\langle \Psi_{SPIGS} | \hat{H} | \Psi_{SPIGS} \rangle}{\langle \Psi_{SPIGS} | \Psi_{SPIGS} \rangle} = \int dR_0 \dots dR_{2M} dS dS' p(R_0, \dots, R_{2M}, S, S') E_L(R_0, R_{2M}, S, S') \quad (3.2)$$

where $p(R_0, \dots, R_{2M}, S, S')$ is the same as in (2.10).

With some care, it is also possible to evaluate imaginary time correlation functions, which are connected to the excitation spectrum of the system, but we don't enter the details of these calculations here.

Moreover, as we shall discuss now, it is possible to calculate the single-particle density matrix, which, at zero temperature, is given by:

$$\rho^{(1)}(\vec{r}, \vec{r}') = \int d^3 r_2 \dots d^3 r_N \psi_0^*(\vec{r}, \vec{r}_2, \dots, \vec{r}_N) \psi_0(\vec{r}', \vec{r}_2, \dots, \vec{r}_N) \quad (3.3)$$

As it is well known, (3.3) is the Fourier transform of the distribution function in momentum space and so, from the behavior of $\rho^{(1)}(\vec{r}, \vec{r}')$ for $|\vec{r} - \vec{r}'| \longrightarrow +\infty$, we can say whether ODLRO is present or not in the system.

For an investigation of a probable supersolid state, it is extremely important to be able to evaluate $\rho^{(1)}(\vec{r}, \vec{r}')$ by means of Monte Carlo methods; in fact, it has been demonstrated that, at $T = 0K$, ODLRO is a sufficient condition for observing non-classical inertia effects. In order to evaluate (3.3) with SPIGS method, we proceed as follows: the function

$$\mu(\vec{r}_0, \vec{r}_1, \vec{r}_2, \dots, \vec{r}_N) \stackrel{def}{=} \psi_{SPIGS}(\vec{r}_0, \vec{r}_2, \dots, \vec{r}_N) \psi_{SPIGS}(\vec{r}_1, \vec{r}_2, \dots, \vec{r}_N) \quad (3.4)$$

is non-negative, and so it can be interpreted as a probability density. In a natural way, (3.3) can be rewritten as a mean value weighted according to (3.4):

$$\rho^{(1)}(\vec{r}, \vec{r}') = \int d^3 r_0 \dots d^3 r_N \mu(\vec{r}_0, \vec{r}_1, \vec{r}_2, \dots, \vec{r}_N) \delta(\vec{r} - \vec{r}_0) \delta(\vec{r}' - \vec{r}_1) \quad (3.5)$$

If one uses (2.8), he easily realizes that (3.4) is again formally equal to the Boltzmann weight of a fluid of polymers, but now one of the N polymers with which we were dealing before has been cut into two halves, each having just one shadow variable, one connected to the point \vec{r}_0 , and the other connected to the point \vec{r}_1 . In this way, even (3.5) can be evaluated using a Metropolis algorithm, only slightly different from the one discussed above. In order to optimize the algorithm, we use the same strategy: in our simulation all the polymers have been cut but, for $N-1$ polymers, the two central atoms remain always together, while in one polymer, the two halves are free (or even “encouraged” through a repulsive factor which helps the ergodicity of the random walk) to separate one from the other, with the constraint that the central atoms remain always on the same line; this constraint is useful to avoid normalization problems. In this way we generate an “off-diagonal Monte Carlo dynamics”, which makes possible the evaluation of (3.3).

It should be clear, after this discussion, that SPIGS is a very powerful method in studying, in an “exact” way, the properties of the system; the main problem is the ergodicity of the Metropolis algorithm. By this we mean that exploring all the configurational space of a fluid of polymers requires lots of computational effort. The fact that interactions, as we have seen before, exist only among the atoms belonging to the same time slice is very important, since it makes the computational time to scale linearly with the number of time slices. Besides, the possibility of efficiently parallelizing the algorithm is extremely useful: in fact it is possible to let each node make a statistically independent simulation and, at the end, we take the averages of the quantities evaluated by each single node. Specially in the case of ODLRO calculation in the solid phase, where we have to wait till the two “half polymers” reach a long distance one from the other, parallelization importance is outstanding.

4. Some results: vacancies in the ground state of ^4He

With the SPIGS method we have studied, in the solid phase of Helium, the physics of point defects in the crystal lattice: vacancies. It is known that the presence of defects, both point-defects (vacancies, vacancy-interstitial pairs ...) and extended defects (stacking-faults, stress ...), could couple to the zero point motion of atoms and help the delocalization of particles, creating the conditions for quantum coherence effects to be observed. It has been shown, in fact, that *if* there is a non-zero concentration of vacancies in the ground state of solid ^4He , then ODLRO is present and this can explain the observed “non-classical inertia” effects.

The question whether a finite concentration of vacancies exists, or, in other terms, whether the ground state of solid ^4He in commensurate other incommensurate, is a very difficult one; a Monte Carlo simulation is not able to answer this question in a direct way. The problem is that, in order to let the system relax toward the *true* thermal equilibrium state, one should allow for fluctuations in particle number and number of lattice sites, while a SPIGS simulation is made at a fixed particle number in a fixed simulation box, in which a given crystal lattice fits.

However, SPIGS method allows to investigate many interesting aspects of the physics of vacancies; in fact one is able to study both the commensurate and the incommensurate system, preparing the initial configuration, from which the Metropolis algorithm starts, as N particles occupying the M sites of a perfect crystal lattice which fits the dimensions of the box in which the simulation takes place and respects periodic boundary conditions.

It is clear that if we choose $N=M$ we are dealing with a commensurate state; otherwise, if $N<M$, we are studying a system with vacancies.

We have evaluated the activation energy of vacancies, calculating the difference between the ground state energy of the commensurate “perfect lattice” at a given particle density, and the energy of systems with one, two, three, four and five vacancies at the *same* particle density; we worked with an hexagonal-close-packet (hcp) lattice of 180 sites at the two densities $\rho = 0.031\text{\AA}^{-3}$ and $\rho = 0.0293\text{\AA}^{-3}$ (melting density), and we used the following formula for the activation energy of $n = M - N$ vacancies:

$$\varepsilon(n; \rho) = \left\{ \frac{E(N = M - n; \rho)}{M - n} - \frac{E(N = M; \rho)}{M} \right\} (M - n) \quad (4.1)$$

where $E(N; \rho)$ is the *total* ground state energy of a system of N particles at the density ρ .

We have also studied the system in the presence of an ^3He atom; it is evident from the experiments that a small ^3He concentration influences the non-classical inertia effect and modifies the transition temperature, and so it is interesting to make simulations of a system in which an ^3He atom is present. SPIGS method allows to handle with this situation easily because, although one doesn't know in principle the difference in microscopic correlations induced by the ^3He atom, one can write the shadow trial wave function ignoring the difference between the two isotopes, because the imaginary time propagator $e^{-\hat{H}\tau}$ gives naturally rise to the correct correlations. Here we reports our results:

$$\rho = 0.031\text{\AA}^{-3}$$

N	<i>Pure system</i>	<i>In presence of an ^3He atom</i>
1	21.3 +/- 0.4	21.4 +/- 0.4
2	40.6 +/- 0.6	41.6 +/- 0.2
3	56.9 +/- 0.6	58.9 +/- 0.4
4	73.0 +/- 0.4	73.6 +/- 0.4
5	89.3 +/- 0.5	87.1 +/- 0.5

$$\rho = 0.0293\text{\AA}^{-3}$$

N	<i>Pure system</i>	
<i>1</i>	<i>15.4 +/- 0.8</i>	
<i>2</i>	<i>30.6 +/- 0.8</i>	
<i>3</i>	<i>43.9 +/- 0.8</i>	
<i>4</i>	<i>53.7 +/- 0.8</i>	
<i>5</i>	<i>63.4 +/- 0.7</i>	

Despite of the large statistical errors (which are due to the multiplication for the number of particles in (4.1)), from our results it is quite evident the negligible role of the ^3He atom, which seems not to couple with vacancies (we have not yet results in the system at the melting density in the presence of the ^3He atom); besides, we can see that the dependence of the activation energy from the number of vacancies is systematically sublinear, suggesting the probable existence of an *attractive interaction* among vacancies. In order to investigate further this attractive force, which, physically, could be connected to long-range responses of the crystalline dislocation field, it is possible, in a SPIGS simulation, to observe the Monte Carlo dynamics of vacancies; in fact we have implemented a method which allows us to see where the vacancies are in each configuration explored by the Metropolis algorithm.

This is achieved by dividing the simulation box in Wigner-Seitz cells, centered on the sites of the perfect crystal prepared in the initial configuration, and attributing to a vacancy a site if it is the center of a Wigner-Seitz cell in which no atom is found and no double occupations are found in the nearest neighbor cells. Using these methods, it is possible to “see” the motion (in the Monte Carlo sense) of the vacancies, to evaluate correlations functions among vacancies and so on. Many simulations in order to put light into the physics of vacancies are at work.

Another experiment we are doing is the calculation of the single-particle density matrix in presence of vacancies with SPIGS simulations. Given that vacancies might well be part of the ground state of solid ^4He , we have computed the one-body density matrix in the presence of vacancies with the exact SPIGS method [11]. Computation of $\rho^{(1)}(\vec{r}, \vec{r}')$ is performed, as commented before, by cutting one of the linear polymers at the central monomer and sampling the distance $|\vec{r} - \vec{r}'|$ of the two cut ends. Notice that in SPIGS computations, contrary to the case of PIMC calculations, no exchange moves between polymers have to be performed; this is a great advantage due to ergodicity problems arising from exchange moves. In any case, the calculation of $\rho^{(1)}(\vec{r}, \vec{r}')$ by means of

SPIGS in the solid is computationally very intensive due to the low relaxation (to get converged results one needs more than 10^7 MC steps) and to the large number of degrees of freedom (i.e., coordinates of monomers) as the imaginary time evolution becomes greater. There is also the necessity to compute $\rho^{(1)}(\vec{r}, \vec{r}')$ as a function of τ in order to control the convergence. We have worked with a box which fits $M = 108$ fcc lattice sites and with $N=107$ and $N=106$ so that we have one or two vacancies which corresponds, respectively, to a vacancy concentration of $X_v=0.93\%$ and $X_v=1.89\%$. In Fig. 1 we show the results at density 0.031 \AA^{-3} , which corresponds to a pressure of about 54 bar. $\rho^{(1)}(\vec{r}, \vec{r}')$ has been computed with $\vec{r} - \vec{r}'$ along the nearest neighbor direction ($[110]$ in fcc).

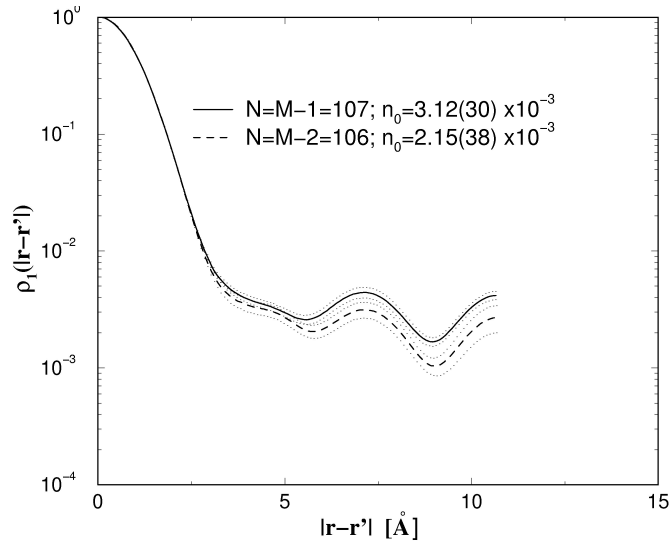


Fig.1 One body density matrix at density 0.031 \AA^{-3} for two different values of concentration of vacancies; we have worked with a box which fits $M = 108$ fcc lattice sites and with $N=107$ and $N=106$ particles so that we have one or two vacancies which corresponds, respectively, to a vacancy concentration of $X_v=0.93\%$ and $X_v=1.89\%$. $\rho^{(1)}(\vec{r}, \vec{r}')$ has been computed with $\vec{r} - \vec{r}'$ along the nearest neighbor direction ($[110]$ in fcc). The dotted curves are shown in order to display the error bars in the calculations.

One can see that $\rho^{(1)}(\vec{r}, \vec{r}')$ develops a plateau for distances greater than about 5 \AA and this is a signature of BEC. We have estimated the condensate fraction by averaging the plateau for distances greater than 5.5 \AA , and the values with their statistical uncertainty are shown in Fig. 1. With SWF it is known that n_0 for the hcp lattice is very similar to the

fcc one [9]. $\rho^{(1)}(\vec{r}, \vec{r}')$ in the plateau region has oscillations and the maxima correspond to multiples of the nearest neighbor distance; this can be interpreted in terms of a sequence of jumps of atoms which make use of the vacancy. This process is distinct from the vacancy-interstitial pairs that were found to be important for the commensurate state in a SWF computation [10]. In order to explore larger distances, recently we have started preliminary computations of $\rho^{(1)}(\vec{r}, \vec{r}')$ with SPIGS also for systems with a bigger number of particles: in Fig.2. we show our very recent results obtained from the simulation which took place in a box fitting $M=256$ fcc lattice sites; we evaluated the one body density matrix for three different values of concentration of vacancies $X_v = 0.78\%$, $X_v = 1.56\%$ and $X_v = 2.34\%$.

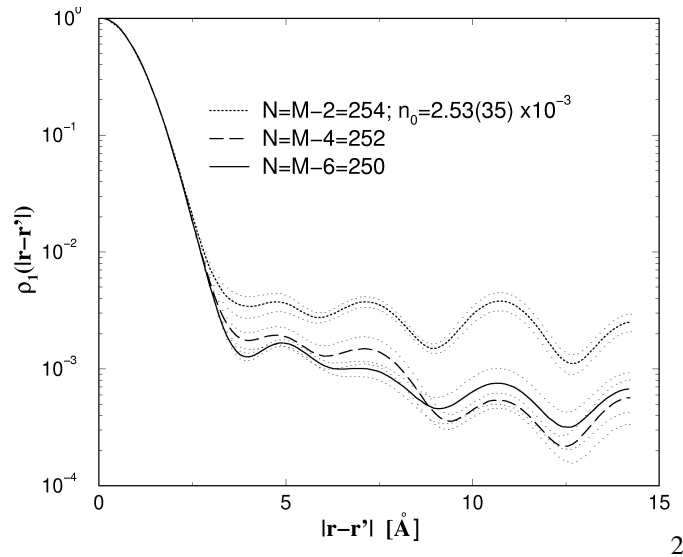


Fig.2 One body density matrix at density 0.031 \AA^{-3} for three different values of concentration of vacancies; we have worked with a box which fits $M=256$ fcc lattice sites and with $N=254$, $N=252$ and $N=250$ particles so that we have two, four or six vacancies which corresponds, respectively, to a vacancy concentration of $X_v = 0.78\%$, $X_v = 1.56\%$ and $X_v = 2.34\%$. $\rho^{(1)}(\vec{r}, \vec{r}')$ has been computed with $\vec{r} - \vec{r}'$ along the nearest neighbor direction ($[110]$ in fcc). The dotted curves are shown in order to display the error bars in the calculations.

One sees from Fig. 2 the persistence of the oscillations around a finite plateau. However the dependence on the value of concentration of vacancies is far from trivial: in fact, in a picture of completely non-interacting vacancies one could expect that each vacancy gives

independently its contribution to the mechanism of mass transport which gives rise to ODLRO and so that n_0 scales with X_v within the statistical uncertainty, while, from Fig. 2, it is evident that such a behaviour breaks completely down above a value of vacancies concentration of about 1%. This behaviour might arise from correlations among vacancies coherently with our results about the activation energies of vacancies.

Therefore vacancies are very efficient in inducing BEC. Using, as an order of magnitude, T_{BEC} of an ideal gas with the effective mass [9] $m=0.35m_{\text{He}}$, we get $T_{\text{BEC}}=11.3(X_v)^{2/3}$; for example, $T_{\text{BEC}}\approx 0.2$ K for $X_v=2.3\times 10^{-3}$ and $T_{\text{BEC}}\approx 10^{-3}$ K for $X_v=10^{-6}$. Therefore we expect supersolidity at low T in bulk solid ^4He if vacancies are present either as part of the ground state or as the non equilibrium effect.

5. Conclusions

We have studied zero-temperature properties of ^4He by means of a new projector Quantum Monte Carlo method, the Shadow Path Integral Ground State (SPIGS). Such a technique is very useful, because it opens the way to study the physics of both the liquid and the solid phase of helium with exact results.

The recent observations of “non-classical rotational inertia” (NCRI) in samples of solid ^4He motivated us to investigate one possible reason for such a behaviour: the presence of vacancies in the system; a finite concentration of vacancies, as we have seen, gives rise to ODLRO and this has been shown to be a sufficient condition for NCRI. This fact makes the study of the physics of vacancies very interesting: correlations, dynamics, activation energies, one body density matrix in presence of vacancies etc.

It is still open the problem whether the true Ground State of the system possesses a finite vacancies concentration or not.

6. Acknowledgments

Some of the results here presented have been obtained by running QMC parallel simulations on the EXADRON (AMD Opetron “Golgi”) Cluster and on the EXADRON (Intel Xeon “Avogadro”) Cluster at CILEA and by using about 17000 cpu hours on these clusters.

References

- [1] G.V. Chester, *Speculations on Bose-Einstein Condensation and Quantum Crystals*. Phys. Rev. A, **2**, 256 (1970)
- [2] A.F. Andreev and I.M. Lifshitz, *Quantum theory of Defects in crystals*. Sov. Phys. JETP, **29**, 1107 (1969)

- [3] E.Kim and M.H.W. Chan, *Probable observation of a supersolid helium phase*. Nature, **427**, 225 (2004); E.Kim and M.H.W. Chan, *Observation of non-classical inertia in solid ^4He confined in porous gold*. J. Low Temp. Phys., **138**, 859 (2005); E.Kim and M.H.W. Chan, *Observation of superflow in solid ^4He* . Science, **305**, 1941 (2004); E.Kim and M.H.W. Chan, *Supersolid properties at high pressure*. Phys. Rev. Lett., **97**, 115302 (2006)
- [4] D.E. Galli and L. Reatto, *The Shadow Path Integral Ground State Method: Study of Confined Solid of Confined Solid ^4He* . J. Low Temp. Phys., **136**, 343 (2004)
- [5] S.A. Vitiello, K. Runge, M.H. Kalos, *Variational Calculations for Solid and Liquid ^4He with a “Shadow” Wave Function*. Phys. Rev. Lett., **60**, 1970 (1988)
- [6] R.A. Aziz, F.R.W. McCourt, C.C.K. Wong, *A new determination of the ground state interatomic potential for He_2* . Mol. Phys., **61**, 1487 (1987)
- [7] D.M. Ceperley, *Path integrals in the theory of condensed helium*. Rev. Mod. Phys., **67** (1995)
- [8] M. Suzuki, *Hybrid exponential product formulas for unbounded operators with possible applications to Monte Carlo Simulations*. Phys. Lett. A, **201**, 425 (1995)
- [9] D.E. Galli and L. Reatto, *Vacancies in solid ^4He and Bose Einstein Condensation*. J. Low Temp. Phys., **124**, 197, (2001)
- [10] D.E. Galli, M. Rossi, L. Reatto, *Bose Einstein Condensation in Solid ^4He* . Phys. Rev. B, **71**, 140506, (2005)
- [11] D.E. Galli, L. Reatto, *Bose Einstein Condensation of Incommensurate Solid ^4He* . Phys. Rev. Lett., **96**, 165301, (2006)